

EMG-Based Volitional Torque Estimation in Functional Electrical Stimulation Control

Hossein Kavianirad
*Dep. of Electrical and
 Computer Engineering*

Technical University of Munich
 Munich, Germany
 hossein.kavianirad@tum.de

Satoshi Endo
*Dep. of Electrical and
 Computer Engineering*

Technical University of Munich
 Munich, Germany
 s.endo@tum.de

Thierry Keller
TECNALIA

*Basque Research and
 Technology Alliance (BRTA)*
 San Sebastian, Spain
 thierry.keller@tecnalia.com

Sandra Hirche
*Dep. of Electrical and
 Computer Engineering*

Technical University of Munich
 Munich, Germany
 hirche@tum.de

Abstract—Functional electrical stimulation (FES) applies electrical pulses to muscle fibers through the skin for assisting functional movements in patients with motor disability. Muscle activity feedback such as volitional Electromyography (vEMG) can optimize the performance of the FES system in both rehabilitation or activity of daily living (ADL), however, artifacts caused by simultaneous use of FES and EMG on the same muscles contaminate the EMG signal. This paper, using an adaptive filter, aims to investigate the estimation of the volitional torque from filtered vEMG. Based on this estimation, the usability and performance of the adaptive filter for estimating volitional torque are studied on 5 healthy participants and we show that this filter can be used for volitional torque estimation. In the next step, it is shown how this map can be used in closed-loop FES control for estimating volitional torque.

Index Terms—FES, EMG, rehabilitation, human-machine interaction, closed-loop control, human-in-the-loop.

I. INTRODUCTION

Functional electrical stimulation (FES) is a neuromuscular stimulation technique that artificially activates muscles, for assisting functional movements in patients with motor disability. By applying electrical stimulation to muscle fibers through the skin, the muscles contract and produce a movement and the technique can be applied for goal-directed functional tasks. The simultaneous limb motion with the electrical activation induced by FES is known to be beneficial for rehabilitation of individuals who have had a stroke or a spinal cord injury to regain their ability to walk, reach, and grasp in their activities of daily living (ADL) [1], [2]. However, actuating the human neuromuscular system with FES for functional tasks is non-trivial, and the FES control design faces several challenges, such as being time-variant, nonlinear, and participant-specific. For instance, activation and contraction dynamics are nonlinear, and muscle fatigue effect is time-variant. A part from that human voluntary movement can affect the performance of the control system, especially, if this involvement is considered as unknown disturbance [3], [4]. Thus, predicting the intention of patients and having feedback from muscle activities can alleviate some of the control challenges and optimise the control performance. Electromyography (EMG), for instance, can be used to extract information about voluntary and involuntary

This research is supported by the European Research Council (ERC) Consolidator Grant “Safe data-driven control for human-centric systems (CO-MAN)” under grant agreement no 864686, and by the European Union’s Horizon 2020 research and innovation programme ReHyb under grant agreement no 87176.

muscle activities [5], [6], and it can be used for intention estimation of movements, including the joint torque acting on the limb [7]–[9]. Translationally, EMG signal can be used to estimate the fatigue state of the muscle and it includes information regarding the recruitment of different types of muscle fibers [10].

To have access to the EMG-based user intention for FES control, (near) real-time processing and analysis of EMG signal are crucial. However, combining FES and EMG on the same muscles introduces an additional challenge. For instance, electrical artifact caused by FES stimulation contaminates the EMG reading [11]–[13]. The artifact obscures the underlying EMG signal, namely volitional EMG (vEMG), generated by the muscle itself. As a result, for efficiently carrying out simultaneous use of FES and EMG in the system, EMG signal in presence of the FES should be processed.

Various hardware- and software-based and offline and online methods for extracting vEMG from raw EMG signal contaminated by FES can be found in the literature [11], [13]–[15]. Blanking windows, band-pass, and comb filters are among commonly used methods [16]–[18]. These methods are easy to implement and suitable for filtering out stationary artifacts. However, due to FES characteristics change (i.e. variation in amplitude, width, or frequency of the stimulation) in most FES usage scenarios such as FES control, the artifact contaminating the EMG signal is non-stationary. Moreover, methods such as blanking window [16] which ignores the transient stimulation part of artifacts, lasting only for a short while, cause loss of data during filtering.

More advanced methods such as Empirical Mode Decomposition with Notch filtering for removing FES artifacts and data-driven vEMG extraction algorithm are studied in [19] and [15], respectively. [11] and [13] suggested an adaptive filter which is able to filter out the non-stationary artifact and extract the vEMG. [11] combined hardware-based shut-down circuit alongside a software-based adaptive filter to eliminate artifacts (transient stimulation and FES-induced muscle response) from the EMG signal. [13] investigated software-based adaptive filtering capable of removing artifacts and extracting vEMG from raw EMG signal. For showing the performance of the proposed filter, they artificially added the artifact to the vEMG in simulation and used Comb and the proposed adaptive filter and they showed that the vEMG extracted from raw EMG by adaptive filter in comparison with comb filter is more coherent with original vEMG.

Following this evaluation, the authors designed and tested a proportional EMG-controlled FES system in which FES intensity is proportional to extracted vEMG.

In this paper, we will investigate the estimation of volitional torque (τ_v) generated by the muscles from the EMG signal. For this, we use the adaptive filter to remove artifacts and extract the vEMG from raw EMG signal, then we will evaluate τ_v -vEMG map. In recent works, such as [13], the performance of the filter is evaluated based on artificially adding and then filtering out the FES artifact, however, in this paper we will evaluate the performance of the adaptive filter by investigating the accuracy of the volitional torque estimation based on the learned τ_v -vEMG map. In the aforementioned paper [13], extracted vEMG is used in proportional FES control. However, in the current paper, we estimate the volitional human torque based on filtered EMG signal (vEMG) and this map will be used in the FES control system to estimate the volitional torque of the participants.

II. ADAPTIVE FILTER

A. Filtering FES Artifacts on EMG

When using the FES and EMG simultaneously on the same group of muscles, artifacts generated directly or indirectly by the FES contaminate the EMG signal and obscure the underlying vEMG signal. These artifacts include transient stimulation, post-stimulus voltage decay, and m-wave.

Transient stimulation

FES applies low-current electrical pulses to muscles, and these pulses directly affect the EMG signal recording and cause sharp and large spikes after each stimulation.

Post-stimulus voltage decay

After the initial spike from the transient stimulation, the leftover dissipating charge is called post-stimulus voltage decay. This affects a few signal samples and corrupts readings of the true muscle activities.

M-wave

M-wave is an indirect result of the FES stimulation. Electrical stimulation sent by FES to the muscle fibers evokes neurons innervating them and this coordinated evoked response causes the so-called M-wave artifact. As M-wave is the evoked response from neurons, it includes some useful information such as the number of active motor units, dispersion of their innervation zones, fatigue, etc. Filtering out the m-waves presents some difficulties, as these waves are non-stationary.

Given the effect of these artifacts in presence of the FES, the raw EMG signal requires signal processing for control applications. Fig. 1 depicts the EMG signal with and without FES artifacts after high-pass filtered to remove the drift. The top figures illustrate the EMG signal without any artifacts (vEMG) during volitional wrist movement while the bottom ones show one during wrist movement with active FES. Fig. 1 clearly shows how FES can change the EMG signal: for instance, it changes the order of signal in this test ten times.

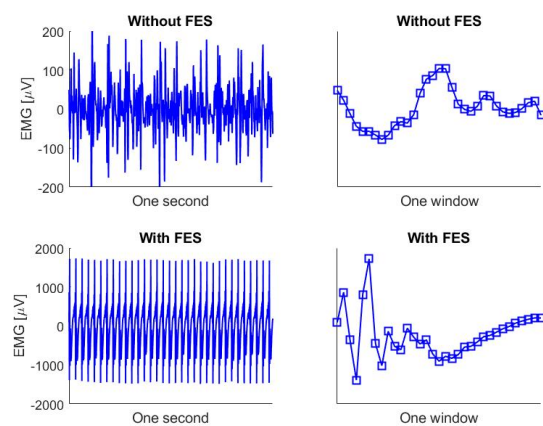


Fig. 1. High-pass filtered EMG signals with and without FES. Top left: voluntary activity without FES (one second), top right: voluntary activity without FES (one window), bottom left: voluntary activity with FES (one second), bottom right: voluntary activity with FES (one window including just one FES stimulation).

B. Adaptive Filter

Real-time processing, filtering, and analysis of EMG signal are required for EMG-based FES control. Furthermore, a closed-loop FES control design entices variable FES intensity (i.e. pulse amplitude, width, and frequency of the stimulation). Therefore, adaptive filtering can be utilised to cope with non-stationary behavior of the artifact. In this part, the adaptation law for the EMG filter based on [11], [13] will be investigated and the experimental results which show the performance of the filter will be shown in the next section.

In adaptive filtering, apart from considering N_s recent EMG samples which we call it current window of data, we consider N_w previous windows (each of which has N_s sample) in order to drive an adaptive law for the filter based on the history of the signal. To align the muscle responses in each frame (one window of data), N_s is considered as the number of sampling between each FES pulse (ratio of EMG frequency to FES frequency). Moreover, different N_w can be considered in this method to investigate the effect of this parameter; indeed, this parameter shows the history of the signal taken into account in adaptive filtering. It should be noted that if the only previous window is taken into account ($N_w=1$) then the result of the adaptive filter is identical to the Comb filter.

The filter is designed to predict the present frame artifacts (EMG signal without volitional activity) from a linear combination of foregoing N_w frames. Fig. 2 illustrates the prediction of the current frame based on previous signal frames. Therefore, subtracting this predicted frame from the current frame will leave a residual signal which shows vEMG.

Filtered signal can be written as (1)

$$y_f = y - y_p \quad (1)$$

where y_f , y , and y_p are the filtered, raw, and predicted signal in the current frame, respectively ($N_s \times 1$ vector).

As described before, we predict the present frame artifacts based on the linear combination of foregoing N_w frames (Fig. 2)

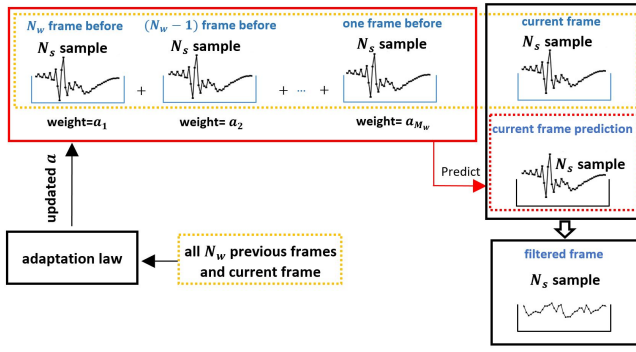


Fig. 2. Adaptive filter schematic diagram. In adaptive filter N_w frames each of which includes N_s sample are considered, based on these frames, artifacts of the current frame are predicted and the difference between the current frame and prediction of the artifacts of the current frame is considered as a vEMG.

$$y_p = Y^T a \quad (2)$$

where a is weight of previous frames or adaptive vector ($N_w \times 1$ vector) and Y is history matrix ($N_w \times N_s$ matrix including all N_w previous frame raw data).

Given (1) and (2), filtered data can be written as

$$y_f = y - Y^T a \quad (3)$$

Consider cost function as

$$J_w = y_f^T y_f \quad (4)$$

Based on literature [11], [13], [20], when the number of active motor units exceeds 15, vEMG is assumed to be zero mean band-limited Gaussian signal. Given this characteristic of vEMG, for deriving the adaptive law, we try to minimize this J_w

$$dJ_w/da = d(y_f^T y_f)/da = 0 \quad (5)$$

Combining (3) and (5), and calculating the derivative, we can write

$$y^T Y^T + a^T Y Y^T = 0 \quad (6)$$

By transposing the last line in (6), the adaptation law will be derived as follow

$$a = (Y Y^T)^{-1} Y y \quad (7)$$

Therefore, given (3) and (7), the filtered signal can be described as

$$y_f = y - Y^T (Y Y^T)^{-1} Y y \quad (8)$$

III. TORQUE-EMG MAP

A. Experiment Setup

Filtering the EMG signal may effects the accuracy of the muscle torque estimation and performance of the controlled system as some artifacts may remain in the resulting signal or the filter may erroneously remove volitional muscle activities. Thus, it is important to investigate whether the filtered data can accurately represent the underlying muscle activities. In this paper, therefore, the map between filtered EMG signal and volitional wrist torque will be analysed. This map can then be used for volitional torque estimation in FES control.

The experiment setup including a 16-electrode array FES (Tecnalia Research Innovation, Spain), EMG (Noraxon, USA), and the HRX-1 robot which applies torque to the user at the wrist (HumanRobotiX, United Kingdom) as shown in Fig. 3. The HRX-1 robot is used for providing a predefined random sequence of torque levels at the wrist, while it measures the angle of the handle and the interaction torque between the user and the robot at the handle. During the experiment, the participant sat on a chair and placed his/her forearm on the HRX-1 robot as elbow naturally flexed about 90 degrees. The task of the participant was to maintain this pose while FES stimulated the lower arm with specific FES intensity and a robot applied a prescribed constant torque to the wrist for 20 seconds at a time. FES intensity was modulated by means of stimulation amplitude and the pulse frequency and width were set as 30 Hz and $300\mu s$, respectively. For this experiment, there were 6 levels of robot torque and 4 levels of FES intensity, giving a total of 24 conditions. The 6 reference torque levels were chosen evenly from zero to 1.4 N.m and the 4 FES intensity levels were zero (FES 0), 3 mA (FES I), 5 mA (FES II), and 7 mA (FES III). Each condition lasted for 16 second each, 4 seconds was used to ramp to the next torque level.

The participants saw the wrist angle and the target in a simple game (see Fig. 4) on a computer screen (red circle which shows the wrist angle should follow the blue circle which is the desired angle in Fig. 4. The angle of the hand, interaction torque and EMG signals were recorded for analyses.

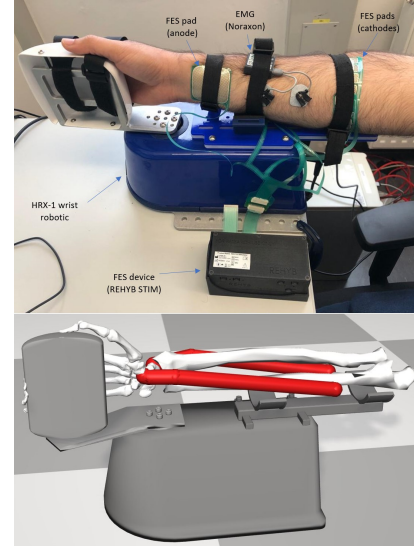


Fig. 3. Experiment setup including FES, EMG, and 1-DoF robot. The below figure depicts the main muscle groups targeted by FES.

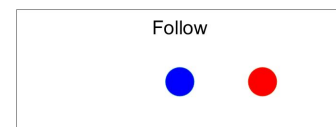


Fig. 4. Experiment game used for filter evaluation and torque-EMG map (blue circle shows the desired target and the red circle shows the current position).

Five healthy individuals participated in this test, their demographic data are summarised in Table I.

TABLE I
PARTICIPANT AGE, GENDER, AND HANDEDNESS

Test No.	Participant*	Gender	Age
1	P1	Female	25
2	P2	Female	22
3	P3	Male	28
4	P4	Male	27
5	P5	Male	25

*All right-handed.

B. Volitional Torque-vEMG Map

To evaluate the performance of the adaptive filter and investigate the possibility and accuracy of the volitional torque estimation based on filtered EMG signal (vEMG), we analyze the map between volitional torque and extracted EMG signal based on five participants' data that we collected in the experiment. As an example, Fig 5 illustrates raw EMG, filtered EMG, and RMS of EMG for healthy participant No.1, FES III. It should be noted that for the adaptive filter 10 previous windows are considered in this section. Furthermore, Fig 6 depicts the RMS of filtered EMG signal and torque for the same person (healthy participant No.1, FES III). To find

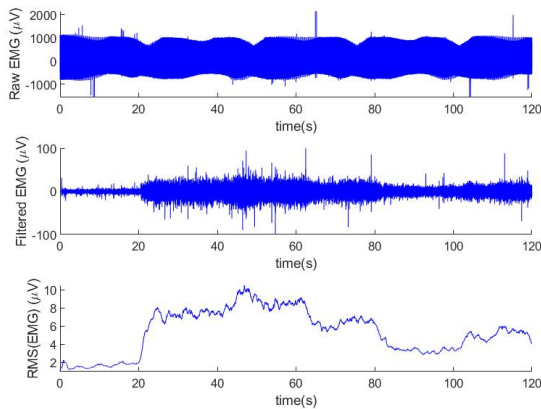


Fig. 5. EMG signal (raw EMG, filtered EMG, and RMS of EMG) for healthy participant No.1, FES III.

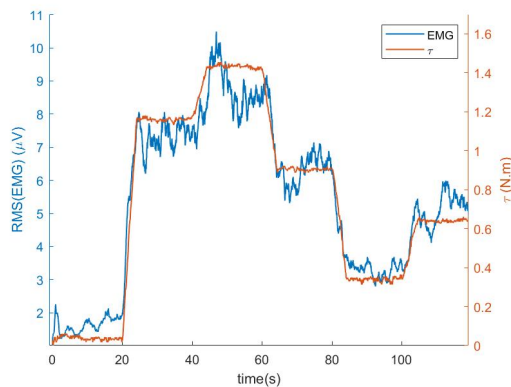


Fig. 6. EMG signal magnitude and τ_v ; healthy participant No.1, FES III.

the appropriate map between volitional torque and vEMG, after implementing the adaptive filter and extracting vEMG from raw signal for all tests and participants, generalized linear regression model with different polynomial degrees for mapping volitional torque and vEMG are compared. Fig 7 compares goodness of fit (based on normalized mean squared error which is equivalent to $1-R^2$) and Akaike Information Criterion (AIC) for different polynomial approximations (the average of five participants is considered). Although goodness of fit enhances by increasing the polynomial degree (from 0.098 to 0.062 when the polynomial degree increases from one to nine), AIC, on the other hand, increases. Given the acceptable goodness of fit for the linear model, its simplicity, and lowest AIC, a linear model between volitional torque and vEMG is considered as an acceptable approximation. Therefore, in the next parts, the characteristics of the linear map will be described. It should be noted that, in evaluating the τ_v -vEMG map, just the constant part of each torque tracking is considered, to do this 10 percent of the start and end of each constant part is not taken into account. Fig 8 illustrates

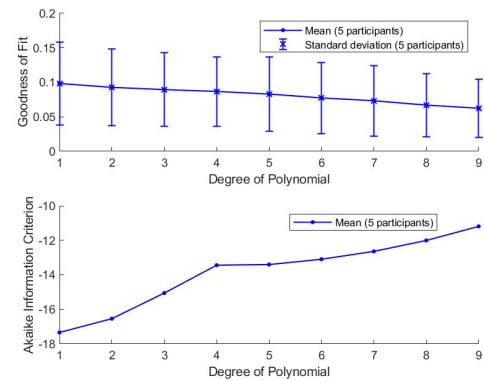


Fig. 7. Goodness of fit (based on normalized mean squared error which is equivalent to $1-R^2$) and AIC for different polynomial approximations (average of five participants are considered).

the mean and standard deviation of volitional torque and filtered EMG signal (vEMG) alongside linear approximation for the τ_v -vEMG map. Five different cases are illustrated in Fig 8; linear approximations are considered for volitional wrist movement (no FES), and wrist movement with FES I, FES II, FES III, and finally one linear approximation for all the EMG signal recorded in FES I, FES II, and FES III. When the filter is active, a correction coefficient which is the fraction of FES 0 and sub-threshold FES (FES I) line slope is considered (for this, line slope in FES 0 and FES I tests are similar in Fig 9).

Finally, Fig 9 compares the slope of the linear approximation line in different participants and different FES intensities, This figure shows that the τ_v -vEMG map is participant-specific as the slope of the linear map is different between different participants. Given the effect of FES intensity on the τ_v -vEMG map, although for different FES intensity the map is not constant, however, in most of the cases, the variation is subtle in comparison to line slope variation in the different participants.

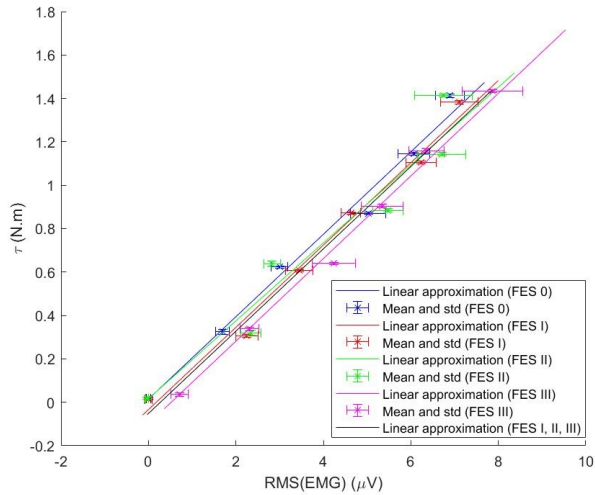


Fig. 8. The τ_v -vEMG map; the mean and standard deviation of EMG signal alongside linear approximation for the map; healthy participant No.1.

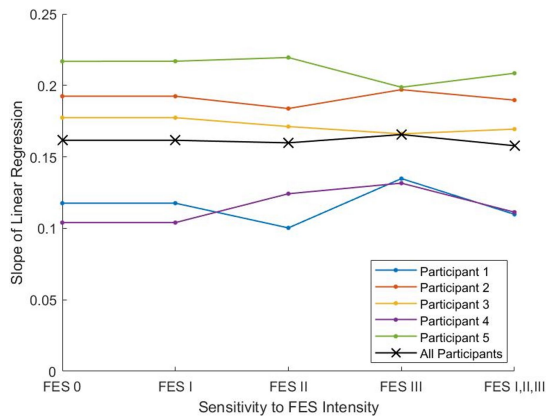


Fig. 9. Comparison of linear approximation line slope in different participants and different FES intensities.

IV. FES CONTROL WITH EMG-BASED VOLITIONAL TORQUE ESTIMATION

A. FES Control

In FES system, joint torque producing functional movement is either a response to the FES stimulation or a result of volitional muscle activity, therefore, apart from having knowledge about neuromuscular response to FES, estimation of the volitional human muscle activity and joint torque can optimize control performance. Fig 10 depicts the control architecture that considered in this study. This control architecture includes calibration, online adaptive filter, volitional torque estimation, and combination of feedforward and feedback FES control. In calibration, for each participant, the static nonlinear function of the discrete-time Hammerstein model [21], [22] and τ_v -vEMG map are learned. They are used in feedforward FES control and volitional torque estimation, respectively.

The setup used for FES control is the same as torque-EMG map experimental setup (Fig 4). In calibration part, different FES intensities in a random sequence are applied to the hand and for each FES intensity, three parts each of which five seconds are considered. In the first part, participant is asked

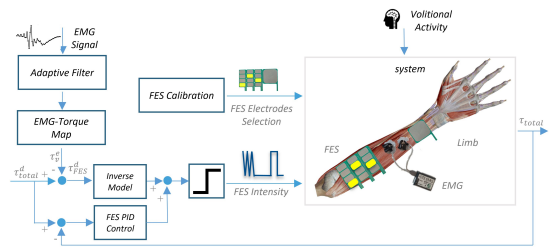


Fig. 10. Control architecture; FES control with EMG-based τ_v estimation.

to be passive while the wrist torque and EMG signal are measured, in the next two five seconds, he/she is asked to follow two desired torque levels (in this test, 0.5 and 1.0 N.m more than measured torque in the first part). Then, the FES-torque and τ_v -vEMG maps are learned which are used in control loop. For showing the effect of τ_v -vEMG map and volitional torque estimation in the control, two possibilities are considered in the test, in one, participant is asked to be passive while the controller try to follow the desired torque (small volitional activity), and in the other part of the test, participant is asked to voluntarily follow the desirable torque as best as possible through the game (considerable volitional activity). The result of the described control architecture tested on participant No.3 in Table I is depicted in Fig 11. Desirable torque (τ_{total}^d), measured torque (τ_{total}), estimated volitional torque based on filtered EMG (τ_v^e), and control input are shown in this figure. Result with the white background (first and last 40 seconds) shows FES control result while the participant did not get feedback from measured torque and was asked to do not voluntary movement as much as possible, the result also confirms this passive aspect as in these parts the estimated volitional torque is relatively small which means the participant was almost voluntary passive.

On the other hand, in the grey area (mid-40 seconds), the participant got feedback about the desirable and measured torque through a game similar to Fig 11 and was asked to voluntarily follow the desired torque as best as possible. As it can be seen in this part, the estimated volitional torque as predicted is increased and as a result, the control input (normalized FES amplitude) reaches the minimum amount while the tracking error is still small.

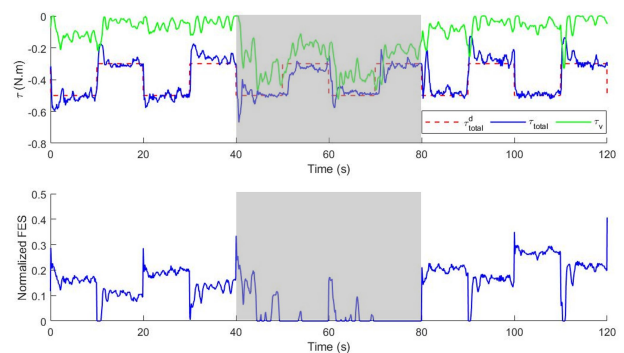


Fig. 11. Control result (P3, Table I): desirable torque (τ_{total}^d), measured torque (τ_{total}), estimated volitional torque based on filtered EMG (τ_v^e), and control input (normalized FES amplitude).

V. CONCLUSION

This paper investigates volitional torque estimation from EMG signal in the combined FES-EMG system. By employing the online adaptive filter, FES artifacts are predicted and removed from raw EMG signal providing filtered vEMG. Then, using the online adaptive filter, the volitional torque-vEMG map is investigated and the usability and performance of the filter for estimating volitional torque are shown. Moreover, it is shown that the linear model is an acceptable approximation for estimating volitional torque from filtered vEMG (average of the goodness of fit for 5 participants=0.098). Finally, FES closed-loop control architecture using the online adaptive filter and the volitional torque-vEMG map for volitional torque estimation is described and tested.

REFERENCES

- [1] N. Alibeji, N. Kirsch, and N. Sharma, "An adaptive low-dimensional control to compensate for actuator redundancy and fes-induced muscle fatigue in a hybrid neuroprosthesis," *Control Engineering Practice*, vol. 59, pp. 204–219, 2017.
- [2] C. Marquez-Chin and M. R. Popovic, "Functional electrical stimulation therapy for restoration of motor function after spinal cord injury and stroke: a review," *Biomedical engineering online*, vol. 19, no. 1, pp. 1–25, 2020.
- [3] F. Resquín, J. Gonzalez-Vargas, J. Ibáñez, F. Brunetti, and J. L. Pons, "Feedback error learning controller for functional electrical stimulation assistance in a hybrid robotic system for reaching rehabilitation," *European journal of translational myology*, vol. 26, no. 3, 2016.
- [4] C.-H. Chang, V. H. Duenas, and A. Sanyal, "Model free nonlinear control with finite-time estimation applied to closed-loop electrical stimulation induced cycling;" in *2020 American Control Conference (ACC)*. IEEE, 2020, pp. 5182–5187.
- [5] Z. Li, D. Guiraud, D. Andreu, A. Gelis, C. Fattal, and M. Hayashibe, "Real-time closed-loop functional electrical stimulation control of muscle activation with evoked electromyography feedback for spinal cord injured patients," *International journal of neural systems*, vol. 28, no. 06, p. 1750063, 2018.
- [6] A. Meilink, B. Hemmen, H. Seelen, and G. Kwakkel, "Impact of emg-triggered neuromuscular stimulation of the wrist and finger extensors of the paretic hand after stroke: a systematic review of the literature," *Clinical rehabilitation*, vol. 22, no. 4, pp. 291–305, 2008.
- [7] P. Xia, J. Hu, and Y. Peng, "Emg-based estimation of limb movement using deep learning with recurrent convolutional neural networks," *Artificial organs*, vol. 42, no. 5, pp. E67–E77, 2018.
- [8] I. M. Khairuddin, S. N. Sidek, A. P. A. Majeed, M. A. M. Razman, A. A. Puzi, and H. M. Yusof, "The classification of movement intention through machine learning models: the identification of significant time-domain emg features," *PeerJ Computer Science*, vol. 7, p. e379, 2021.
- [9] D. Farina, N. Jiang, H. Rehbaum, A. Holobar, B. Graimann, H. Dietl, and O. C. Aszmann, "The extraction of neural information from the surface emg for the control of upper-limb prostheses: emerging avenues and challenges," *IEEE Transactions on Neural Systems and Rehabilitation Engineering*, vol. 22, no. 4, pp. 797–809, 2014.
- [10] M. Cifrek, V. Medved, S. Tonković, and S. Ostojčić, "Surface emg based muscle fatigue evaluation in biomechanics," *Clinical biomechanics*, vol. 24, no. 4, pp. 327–340, 2009.
- [11] S. Sennels, F. Biering-Sorensen, O. T. Andersen, and S. D. Hansen, "Functional neuromuscular stimulation controlled by surface electromyographic signals produced by volitional activation of the same muscle: adaptive removal of the muscle response from the recorded emg-signal," *IEEE Transactions on Rehabilitation Engineering*, vol. 5, no. 2, pp. 195–206, 1997.
- [12] A. Zhou, S. R. Santacruz, B. C. Johnson, G. Alexandrov, A. Moin, F. L. Burghardt, J. M. Rabaey, J. M. Carmena, and R. Muller, "A wireless and artefact-free 128-channel neuromodulation device for closed-loop stimulation and recording in non-human primates," *Nature biomedical engineering*, vol. 3, no. 1, pp. 15–26, 2019.
- [13] B. A. Osuagwu, E. Whicher, and R. Shirley, "Active proportional electromyogram controlled functional electrical stimulation system," *Scientific reports*, vol. 10, no. 1, pp. 1–15, 2020.
- [14] Y. Muraoka, "Development of an emg recording device from stimulation electrodes for functional electrical stimulation." *Frontiers of medical and biological engineering: the international journal of the Japan Society of Medical Electronics and Biological Engineering*, vol. 11, no. 4, pp. 323–333, 2002.
- [15] Y. Zhou, Z. Bi, M. Ji, S. Chen, W. Wang, K. Wang, B. Hu, X. Lü, and Z. Wang, "A data-driven volitional emg extraction algorithm during functional electrical stimulation with time variant parameters," *IEEE Transactions on Neural Systems and Rehabilitation Engineering*, vol. 28, no. 5, pp. 1069–1080, 2020.
- [16] M. Knaflitz and R. Merletti, "Suppression of stimulation artifacts from myoelectric-evoked potential recordings," *IEEE Transactions on Biomedical Engineering*, vol. 35, no. 9, pp. 758–763, 1988.
- [17] C. Frigo, M. Ferrarin, W. Frasson, E. Pavan, and R. Thorsen, "Emg signals detection and processing for on-line control of functional electrical stimulation," *Journal of Electromyography and Kinesiology*, vol. 10, no. 5, pp. 351–360, 2000.
- [18] Y. Li, J. Chen, and Y. Yang, "A method for suppressing electrical stimulation artifacts from electromyography," *International journal of neural systems*, vol. 29, no. 06, p. 1850054, 2019.
- [19] R. Pilkar, M. Yarossi, A. Ramanujam, V. Rajagopalan, M. B. Bayram, M. Mitchell, S. Canton, and G. Forrest, "Application of empirical mode decomposition combined with notch filtering for interpretation of surface electromyograms during functional electrical stimulation," *IEEE transactions on Neural Systems and Rehabilitation Engineering*, vol. 25, no. 8, pp. 1268–1277, 2016.
- [20] C. J. De Luca, "Physiology and mathematics of myoelectric signals," *IEEE Transactions on Biomedical Engineering*, no. 6, pp. 313–325, 1979.
- [21] X. Tu, X. Zhou, J. Li, C. Su, X. Sun, H. Han, X. Jiang, and J. He, "Iterative learning control applied to a hybrid rehabilitation exoskeleton system powered by pam and fes," *Cluster Computing*, vol. 20, no. 4, pp. 2855–2868, 2017.
- [22] C. L. Lynch and M. R. Popovic, "Functional electrical stimulation," *IEEE control systems magazine*, vol. 28, no. 2, pp. 40–50, 2008.